

First calculation of Mueller Navelet jets at LHC at a complete NLL BFKL order

Samuel Wallon

Université Pierre et Marie Curie
and
Laboratoire de Physique Théorique
CNRS / Université Paris Sud
Orsay

Seminar “High Energy Physics”,
Department of Physics & Astronomy, University College London

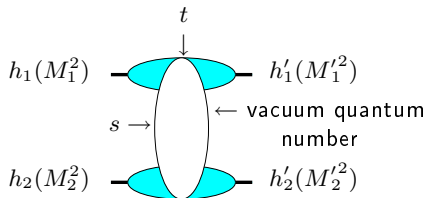
London, April 15th 2011

in collaboration with

D. Colferai (Firenze), F. Schwennsen (DESY), L. Szymanowski (SINS, Warsaw)

Motivations

- One of the important longstanding theoretical questions raised by QCD is its behaviour in the perturbative **Regge** limit $s \gg -t$
- Based on theoretical grounds, one should identify and test suitable observables in order to test this peculiar dynamics



hard scales: $M_1^2, M_2^2 \gg \Lambda_{QCD}^2$ or $M_1'^2, M_2'^2 \gg \Lambda_{QCD}^2$ or $t \gg \Lambda_{QCD}^2$
 where the t -channel exchanged state is the so-called **hard Pomeron**

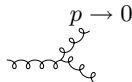
How to test QCD in the perturbative Regge limit?

What kind of observable?

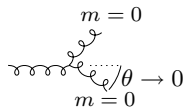
- perturbation theory should be applicable:

selecting external or internal probes with transverse sizes $\ll 1/\Lambda_{QCD}$ (*hard* γ^* , *heavy meson* (J/Ψ , Υ), *energetic forward jets*) or by choosing large t in order to provide the hard scale.

- governed by the "*soft*" perturbative dynamics of QCD



and *not* by its *collinear* dynamics



\implies select semi-hard processes with $s \gg p_{T_i}^2 \gg \Lambda_{QCD}^2$ where $p_{T_i}^2$ are typical transverse scale, **all of the same order**.

How to test QCD in the perturbative Regge limit?

Some examples of processes

- **inclusive**: DIS (HERA), diffractive DIS, total $\gamma^*\gamma^*$ cross-section (LEP, ILC)
- **semi-inclusive**: forward jet and π^0 production in DIS, Mueller-Navelet double jets, diffractive double jets, high p_T central jet, in hadron-hadron colliders (Tevatron, LHC)
- **exclusive**: exclusive meson production in DIS, double diffractive meson production at e^+e^- colliders (ILC), ultraperipheral events at LHC (Pomeron, Odderon)

The specific case of QCD at large s

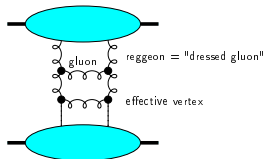
QCD in the perturbative Regge limit

- Small values of α_S (perturbation theory applies due to hard scales) can be compensated by large $\ln s$ enhancements. \Rightarrow resummation of $\sum_n (\alpha_S \ln s)^n$ series (Balitski, Fadin, Kuraev, Lipatov)

$$\mathcal{A} = \underbrace{\text{Diagram 1}}_{\sim s} + \left(\underbrace{\text{Diagram 2}}_{\sim s (\alpha_S \ln s)} + \underbrace{\text{Diagram 3}}_{\sim s (\alpha_S \ln s)^2} + \dots \right) + \left(\underbrace{\text{Diagram 4}}_{\sim s (\alpha_S \ln s)^2} + \dots \right) + \dots$$

The diagrams show a series of terms in a perturbative expansion. The first term is a tree-level diagram with two external lines and a single gluon exchange, labeled $\sim s$. The second term is a sum of diagrams with two gluon exchanges, labeled $\sim s (\alpha_S \ln s)$. The third term is a sum of diagrams with three gluon exchanges, labeled $\sim s (\alpha_S \ln s)^2$. Ellipses indicate higher-order terms.

- this results in the effective BFKL ladder

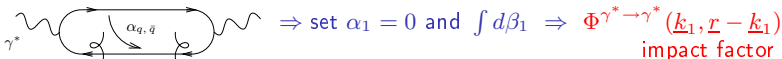


$$\Rightarrow \sigma_{tot}^{h_1 h_2 \rightarrow anything} = \frac{1}{s} \text{Im} \mathcal{A} \sim s^{\alpha_{\mathbb{P}}(0) - 1}$$

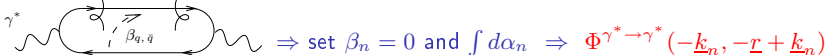
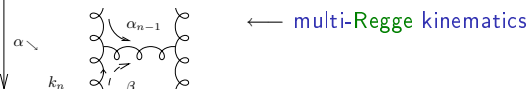
with $\alpha_{\mathbb{P}}(0) - 1 = C \alpha_S$ ($C > 0$) **Leading Log Pomeron**
 Balitsky, Fadin, Kuraev, Lipatov

Opening the boxes: Impact representation $\gamma^* \gamma^* \rightarrow \gamma^* \gamma^*$ as an example

- **Sudakov** decomposition: $k_i = \alpha_i p_1 + \beta_i p_2 + k_{\perp i}$ ($p_1^2 = p_2^2 = 0$, $2p_1 \cdot p_2 = s$)
- write $d^4 k_i = \frac{s}{2} d\alpha_i d\beta_i d^2 k_{\perp i}$ ($\underline{k} = \text{Eucl.} \leftrightarrow k_{\perp} = \text{Mink.}$)
- t -channel gluons have **non-sense** polarizations at large s : $\epsilon_{NS}^{up/down} = \frac{2}{s} p_{2/1}$



$$\mathcal{M} = \frac{is}{(2\pi)^2} \int \frac{d^2 \underline{k}}{\underline{k}^2} \Phi^{up}(\underline{k}, \underline{r} - \underline{k}) \int \frac{d^2 \underline{k}'}{\underline{k}'^2} \Phi^{down}(-\underline{k}', -\underline{r} + \underline{k}') \\ \times \int_{\delta - i\infty}^{\delta + i\infty} \frac{d\omega}{2\pi i} \left(\frac{s}{s_0}\right)^\omega G_\omega(\underline{k}, \underline{k}', \underline{r})$$



higher order corrections

- Higher order corrections to BFKL kernel are known at NLL order (Lipatov Fadin; Camici, Ciafaloni), now for arbitrary impact parameter $\alpha_S \sum_n (\alpha_S \ln s)^n$ resummation

- impact factors are known in some cases at NLL

- $\gamma^* \rightarrow \gamma^*$ at $t = 0$ (Bartels, Colferai, Gieseke, Kyrielleis, Qiao)

- forward jet production (Bartels, Colferai, Vacca)

- $\gamma_L^* \rightarrow \rho_L$ in the forward limit (Ivanov, Kotsky, Papa)

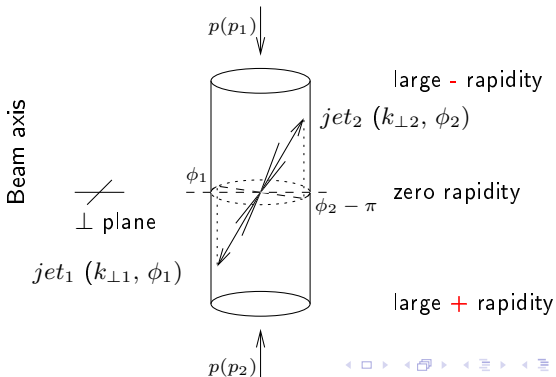
note: for exclusive processes, some transitions may start at twist3, for which almost nothing is known. The first computation of the $\gamma_T^* \rightarrow \rho_T$ twist 3 transition at LL has been performed only recently

I. V. Anikin, D. Y. Ivanov, B. Pire, L. Szymanowski and S. W.
Phys. Lett. B 688:154-167, 2010; Nucl. Phys. B 828:1-68, 2010.

Mueller-Navelet jets: Basics

Mueller Navelet jets

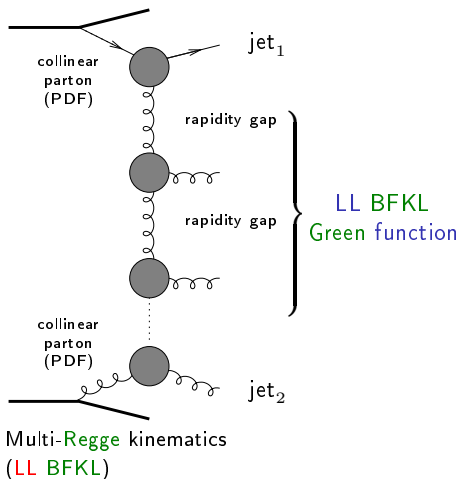
- Consider two jets (hadron packet within a narrow cone) separated by a large rapidity, i.e. each of them almost fly in the direction of the hadron “close” to it, and with very similar transverse momenta
- in a pure LO collinear treatment, these two jets should be emitted back to back at leading order: $\Delta\phi - \pi = 0$ ($\Delta\phi = \phi_1 - \phi_2 =$ relative azimuthal angle) and $k_{\perp 1} = k_{\perp 2}$. There is no phase space for (untagged) emission between them



Mueller-Navelet jets at LL fails

Mueller Navelet jets at LL BFKL

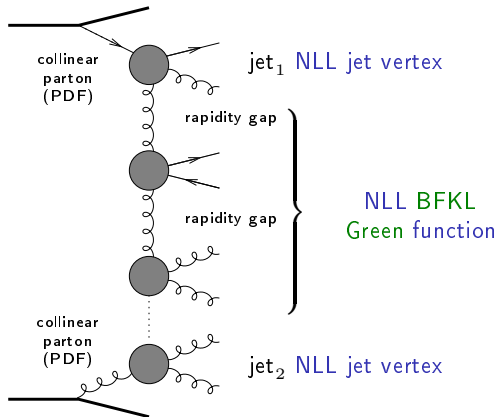
- in LL BFKL ($\sim \sum (\alpha_s \ln s)^n$), emission between these jets \rightarrow **strong decorrelation** between the relative azimuthal angle jets, incompatible with $p\bar{p}$ Tevatron collider data
- a collinear treatment at next-to-leading order (NLO) can describe the data
- important issue: non-conservation of energy-momentum along the BFKL ladder. A BFKL-based Monte Carlo combined with e-m conservation improves dramatically the situation (Orr and Stirling)



Studies at LHC: Mueller-Navelet jets

Mueller Navelet jets at NLL BFKL

- up to now, the subseries $\alpha_s \sum (\alpha_s \ln s)^n$ NLL was included only in the exchanged Pomeron state, and not inside the jet vertices Sabio Vera, Schwennsen Marquet, Royon
- the common belief was that these corrections should not be important

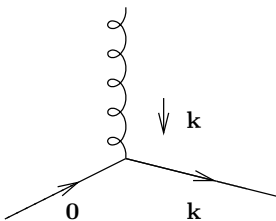


Quasi Multi-Regge kinematics (here for NLL BFKL)

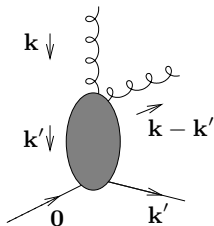
Jet vertex: LL versus NLL

 $\mathbf{k}, \mathbf{k}' =$ Euclidian two dimensional vectors

LL jet vertex:



NLL jet vertex:



Jet vertex: jet algorithms

Jet algorithms

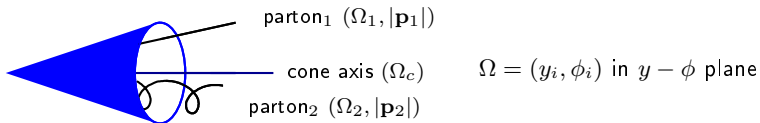
- a jet algorithm should be IR safe, both for soft and collinear singularities
- the most common jet algorithm are:
 - k_t algorithms (IR safe but time consuming for multiple jets configurations)
 - cone algorithm (not IR safe in general; can be made IR safe at NLO: Ellis, Kunszt, Soper)

Jet vertex: jet algorithms

Cone jet algorithm at NLO (Ellis, Kunszt, Soper)

- Should partons ($|\mathbf{p}_1|, \phi_1, y_1$) and ($|\mathbf{p}_2|, \phi_2, y_2$) combined in a single jet?
 $|\mathbf{p}_i|$ = transverse energy deposit in the calorimeter cell i of parameter $\Omega = (y_i, \phi_i)$ in $y - \phi$ plane
- define transverse energy of the jet: $p_J = |\mathbf{p}_1| + |\mathbf{p}_2|$
- jet axis:

$$\Omega_c \begin{cases} y_J = \frac{|\mathbf{p}_1| y_1 + |\mathbf{p}_2| y_2}{p_J} \\ \phi_J = \frac{|\mathbf{p}_1| \phi_1 + |\mathbf{p}_2| \phi_2}{p_J} \end{cases}$$



If distances $|\Omega_i - \Omega_c|^2 \equiv (y_i - y_c)^2 + (\phi_i - \phi_c)^2 < R^2$ ($i = 1$ and $i = 2$)

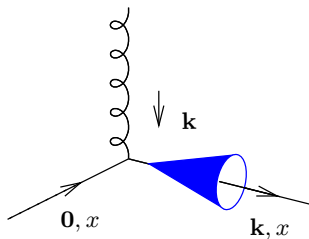
\implies partons 1 and 2 are in the same cone Ω_c

combined condition: $|\Omega_1 - \Omega_2| < \frac{|\mathbf{p}_1| + |\mathbf{p}_2|}{\max(|\mathbf{p}_1|, |\mathbf{p}_2|)} R$

Jet vertex: LL versus NLL and jet algorithms

LL jet vertex and cone algorithm

$\mathbf{k}, \mathbf{k}' =$ Euclidian two dimensional vectors



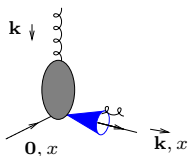
$$\mathcal{S}_J^{(2)}(k_{\perp}; x) = \delta\left(1 - \frac{x_J}{x}\right) |\mathbf{k}| \delta^{(2)}(\mathbf{k} - \mathbf{k}_J)$$

Jet vertex: LL versus NLL and jet algorithms

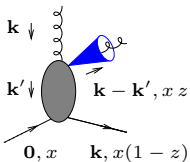
NLL jet vertex and cone algorithm

 $\mathbf{k}, \mathbf{k}' =$ Euclidian two dimensional vectors

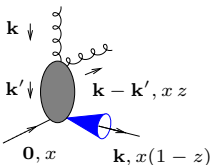
$$\mathcal{S}_J^{(3,\text{cone})}(\mathbf{k}', \mathbf{k} - \mathbf{k}', xz; x) =$$



$$\mathcal{S}_J^{(2)}(\mathbf{k}, x) \Theta \left(\left[\frac{|\mathbf{k} - \mathbf{k}'| + |\mathbf{k}'|}{\max(|\mathbf{k} - \mathbf{k}'|, |\mathbf{k}'|)} R_{\text{cone}} \right]^2 - [\Delta y^2 + \Delta \phi^2] \right)$$



$$+ \mathcal{S}_J^{(2)}(\mathbf{k} - \mathbf{k}', xz) \Theta \left([\Delta y^2 + \Delta \phi^2] - \left[\frac{|\mathbf{k} - \mathbf{k}'| + |\mathbf{k}'|}{\max(|\mathbf{k} - \mathbf{k}'|, |\mathbf{k}'|)} R_{\text{cone}} \right]^2 \right)$$



$$+ \mathcal{S}_J^{(2)}(\mathbf{k}', x(1-z)) \Theta \left([\Delta y^2 + \Delta \phi^2] - \left[\frac{|\mathbf{k} - \mathbf{k}'| + |\mathbf{k}'|}{\max(|\mathbf{k} - \mathbf{k}'|, |\mathbf{k}'|)} R_{\text{cone}} \right]^2 \right),$$

Mueller-Navelet jets at NLL and finiteness

Using a IR safe jet algorithm, Mueller-Navelet jets at NLL are finite

- UV sector:
 - the NLL impact factor contains UV divergencies $1/\epsilon$
 - they are absorbed by the renormalization of the coupling: $\alpha_S \longrightarrow \alpha_S(\mu_R)$
- IR sector:
 - PDF have IR collinear singularities: pole $1/\epsilon$ at LO
 - these collinear singularities can be compensated by collinear singularities of the two jets vertices and the real part of the BFKL kernel
 - the remaining collinear singularities compensate exactly among themselves
 - soft singularities of the real and virtual BFKL kernel, and of the jets vertices compensates among themselves

This was shown for both quark and gluon initiated vertices (Bartels, Colferai, Vacca)

Master formulas

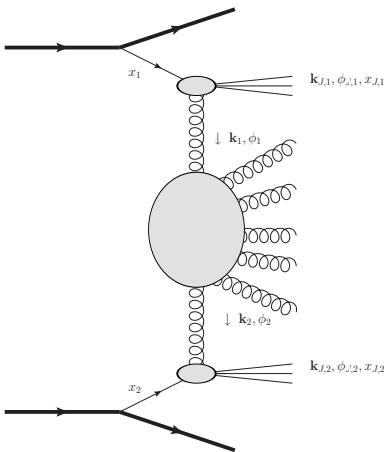
 k_T -factorized differential cross-section

$$\frac{d\sigma}{d|\mathbf{k}_{J,1}| d|\mathbf{k}_{J,2}| dy_{J,1} dy_{J,2}} = \int d\phi_{J,1} d\phi_{J,2} \int d^2\mathbf{k}_1 d^2\mathbf{k}_2$$

$$\times \Phi(\mathbf{k}_{J,1}, x_{J,1}, -\mathbf{k}_1)$$

$$\times G(\mathbf{k}_1, \mathbf{k}_2, \hat{s})$$

$$\times \Phi(\mathbf{k}_{J,2}, x_{J,2}, \mathbf{k}_2)$$



$$\text{with } \Phi(\mathbf{k}_{J,2}, x_{J,2}, \mathbf{k}_2) = \int dx_2 f(x_2) V(\mathbf{k}_2, x_2) \quad f \equiv \text{PDF} \quad x_J = \frac{|\mathbf{k}_J|}{\sqrt{s}} e^{y_J}$$

Master formulas

Angular coefficients

$$C_m \equiv \int d\phi_{J,1} d\phi_{J,2} \cos(m(\phi_{J,1} - \phi_{J,2} - \pi)) \\ \times \int d^2\mathbf{k}_1 d^2\mathbf{k}_2 \Phi(\mathbf{k}_{J,1}, x_{J,1}, -\mathbf{k}_1) G(\mathbf{k}_1, \mathbf{k}_2, \hat{s}) \Phi(\mathbf{k}_{J,2}, x_{J,2}, \mathbf{k}_2).$$

- $m = 0 \implies$ cross-section

$$\frac{d\sigma}{d|\mathbf{k}_{J,1}| d|\mathbf{k}_{J,2}| dy_{J,1} dy_{J,2}} = C_0$$

- $m > 0 \implies$ azimuthal decorrelation

$$\langle \cos(m\varphi) \rangle \equiv \langle \cos(m(\phi_{J,1} - \phi_{J,2} - \pi)) \rangle = \frac{C_m}{C_0}$$

Master formulas in conformal variables

Rely on LL BFKL eigenfunctions

- LL BFKL eigenfunctions: $E_{n,\nu}(\mathbf{k}_1) = \frac{1}{\pi\sqrt{2}} (\mathbf{k}_1^2)^{i\nu - \frac{1}{2}} e^{in\phi_1}$
- decompose Φ on this basis
- use the known LL eigenvalue of the BFKL equation on this basis:

$$\omega(n, \nu) = \bar{\alpha}_s \chi_0(|n|, \frac{1}{2} + i\nu)$$

$$\text{with } \chi_0(n, \gamma) = 2\Psi(1) - \Psi(\gamma + \frac{n}{2}) - \Psi(1 - \gamma + \frac{n}{2})$$

$$(\Psi(x) = \Gamma'(x)/\Gamma(x), \bar{\alpha}_s = N_c \alpha_s / \pi)$$

- \implies master formula:

$$C_m = (4 - 3\delta_{m,0}) \int d\nu C_{m,\nu}(|\mathbf{k}_{J,1}|, x_{J,1}) C_{m,\nu}^*(|\mathbf{k}_{J,2}|, x_{J,2}) \left(\frac{\hat{s}}{s_0}\right)^{\omega(m,\nu)}$$

with

$$C_{m,\nu}(|\mathbf{k}_J|, x_J) = \int d\phi_J d^2\mathbf{k} dx f(x) V(\mathbf{k}, x) E_{m,\nu}(\mathbf{k}) \cos(m\phi_J)$$

- at NLL, same master formula: just change $\omega(m, \nu)$ and V

BFKL Green's function at NLL

NLL Green's function: rely on LL BFKL eigenfunctions

- NLL BFKL kernel is not conformal invariant
- LL $E_{n,\nu}$ are not anymore eigenfunction
- this can be overcome by considering the eigenvalue as an operator with a part containing $\frac{\partial}{\partial \nu}$
- it acts on the impact factor

$$\omega(n, \nu) = \bar{\alpha}_s \chi_0 \left(|n|, \frac{1}{2} + i\nu \right) + \bar{\alpha}_s^2 \left[\chi_1 \left(|n|, \frac{1}{2} + i\nu \right) - \frac{\pi b_0}{2N_c} \chi_0 \left(|n|, \frac{1}{2} + i\nu \right) \left\{ \underbrace{-2 \ln \mu_R^2 - i \frac{\partial}{\partial \nu} \ln \frac{C_{n,\nu}(|\mathbf{k}_{J,1}|, x_{J,1})}{C_{n,\nu}(|\mathbf{k}_{J,2}|, x_{J,2})}}_{2 \ln \frac{|\mathbf{k}_{J,1}| \cdot |\mathbf{k}_{J,2}|}{\mu_R^2}} \right\} \right],$$

LL subtraction and s_0

- one sums up $\sum (\alpha_s \ln \hat{s}/s_0)^n + \alpha_s \sum (\alpha_s \ln \hat{s}/s_0)^n$ ($\hat{s} = x_1 x_2 s$)
- at LL s_0 is arbitrary
- natural choice: $s_0 = \sqrt{s_{0,1} s_{0,2}}$ $s_{0,i}$ for each of the scattering objects
 - possible choice: $s_{0,i} = (|\mathbf{k}_J| + |\mathbf{k}_J - \mathbf{k}|)^2$ (Bartels, Colferai, Vacca)
 - but depend on \mathbf{k} , which is integrated over
 - \hat{s} is not an external scale ($x_{1,2}$ are integrated over)

we prefer

$$\left. \begin{aligned} s_{0,1} &= (|\mathbf{k}_{J,1}| + |\mathbf{k}_{J,1} - \mathbf{k}_1|)^2 \rightarrow s'_{0,1} = \frac{x_1^2}{x_{J,1}^2} \mathbf{k}_{J,1}^2 \\ s_{0,2} &= (|\mathbf{k}_{J,2}| + |\mathbf{k}_{J,2} - \mathbf{k}_2|)^2 \rightarrow s'_{0,2} = \frac{x_2^2}{x_{J,2}^2} \mathbf{k}_{J,2}^2 \end{aligned} \right\} \frac{\hat{s}}{s_0} \rightarrow \frac{\hat{s}}{s'_0} = \frac{x_{J,1} x_{J,2} s}{|\mathbf{k}_{J,1}| |\mathbf{k}_{J,2}|} = e^{y_{J,1} - y_{J,2}} \equiv e^Y$$

- $s_0 \rightarrow s'_0$ affects
 - the BFKL NLL Green function
 - the impact factors:

$$\Phi_{\text{NLL}}(\mathbf{k}_i; s'_{0,i}) = \Phi_{\text{NLL}}(\mathbf{k}_i; s_{0,i}) + \int d^2\mathbf{k}' \Phi_{\text{LL}}(\mathbf{k}'_i) \mathcal{K}_{\text{LL}}(\mathbf{k}'_i, \mathbf{k}_i) \frac{1}{2} \ln \frac{s'_{0,i}}{s_{0,i}} \quad (1)$$

- numerical stabilities (non azimuthal averaging of LL subtraction) improved with the choice $s_{0,i} = (\mathbf{k}_i - 2\mathbf{k}_{J,i})^2$ (then replaced by $s'_{0,i}$ after numerical integration)
- (1) can be used to test $s_0 \rightarrow \lambda s_0$ dependence

Collinear improvement at NLL

Collinear improved Green's function at NLL

- one may improve the NLL **BFKL** kernel for $n = 0$ by imposing its compatibility with **DGLAP** in the collinear limit
Salam; Ciafaloni, Colferai
- usual (anti)collinear poles in $\gamma = 1/2 + i\nu$ (resp. $1 - \gamma$) are shifted by $\omega/2$
- one practical implementation:
 - the new kernel $\bar{\alpha}_s \chi^{(1)}(\gamma, \omega)$ with shifted poles replaces
$$\bar{\alpha}_s \chi_0(\gamma, 0) + \bar{\alpha}_s^2 \chi_1(\gamma, 0)$$
 - $\omega(0, \nu)$ is obtained by solving the implicit equation

$$\omega(0, \nu) = \bar{\alpha}_s \chi^{(1)}(\gamma, \omega(0, \nu))$$

for $\omega(n, \nu)$ numerically.

- there is no need for any jet vertex improvement because of the absence of γ and $1 - \gamma$ poles (numerical proof using **Cauchy** theorem "backward")

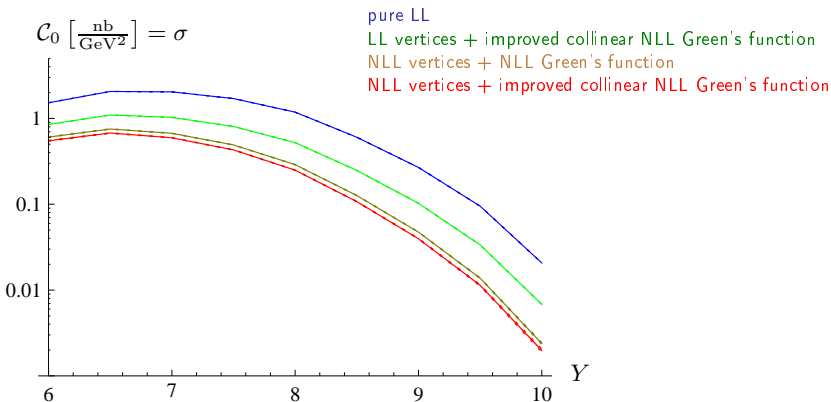
Numerical implementation

In practice

- MSTW 2008 PDFs (available as Mathematica packages)
 - $\mu_R = \mu_F$ (this is imposed by the MSTW 2008 PDFs)
 - two-loop running coupling $\alpha_s(\mu_R^2)$
 - We use a ν grid (with a dense sampling around 0)
 - all numerical calculations are done in Mathematica
 - we use Cuba integration routines (in practice Vegas): precision 10^{-2} for 500.000 max points per integration
 - mapping $|\mathbf{k}| = |\mathbf{k}_J| \tan(\xi\pi/2)$ for \mathbf{k} integrations $\Rightarrow [0, \infty[\rightarrow [0, 1]$
 - although formally the results should be finite, it requires a special grouping of the integrand in order to get stable results
- \implies 14 minimal stable basic blocks to be evaluated numerically

Results: symmetric configuration ($|\mathbf{k}_{J,1}| = |\mathbf{k}_{J,2}| = 35 \text{ GeV}$)

Cross-section



Differential cross section in dependence on Y for $|\mathbf{k}_{J,1}| = |\mathbf{k}_{J,2}| = 35 \text{ GeV}$.
 error bands=errors due to the Monte Carlo integration (2% to 5%)

The effect of NLL vertex correction is very sizeable, comparable with NLL Green's function effects

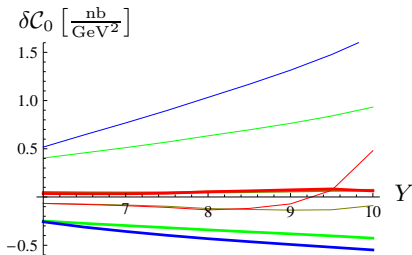
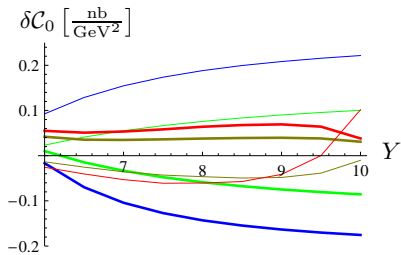
Results: symmetric configuration ($|\mathbf{k}_{J,1}| = |\mathbf{k}_{J,2}| = 35 \text{ GeV}$)Cross-section: stability with respect to $\mu_R = \mu_F$ and s_0 changes

pure LL

LL vertices + improved collinear NLL Green's function

NLL vertices + NLL Green's function

NLL vertices + improved collinear NLL Green's function

Relative effect of changing $\mu_R = \mu_F$
by factors 2 (thick) and 1/2 (thin)Relative effect of changing $\sqrt{s_0}$
by factors 2 (thick) and 1/2 (thin)

Results: symmetric configuration ($|\mathbf{k}_{J,1}| = |\mathbf{k}_{J,2}| = 35 \text{ GeV}$)

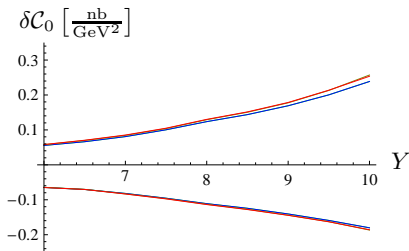
Cross-section: PDF and Monte Carlo errors

pure LL

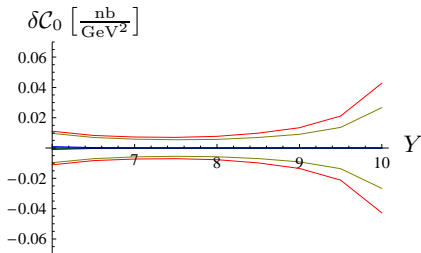
LL vertices + improved collinear NLL Green's function

NLL vertices + NLL Green's function

NLL vertices + improved collinear NLL Green's function



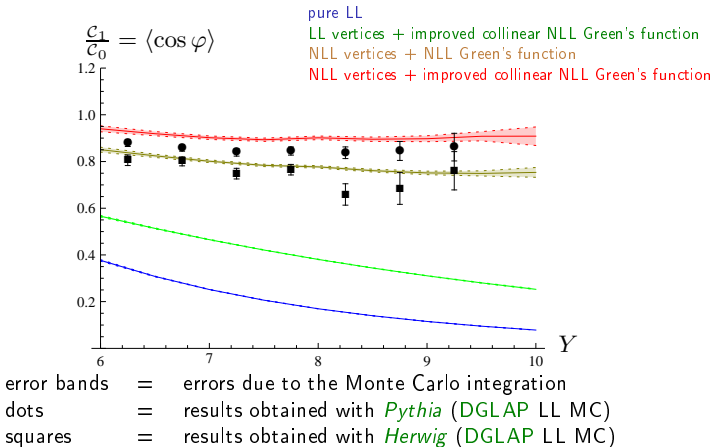
Relative effect of the PDF errors



Relative effect of the Monte Carlo errors

Results: symmetric configuration ($|\mathbf{k}_{J,1}| = |\mathbf{k}_{J,2}| = 35 \text{ GeV}$)

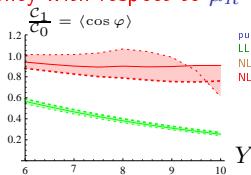
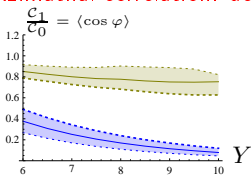
Azimuthal correlation



- LL \rightarrow NLL vertices change results dramatically
- At NLL, the decorrelation is very close to LL DGLAP type of Monte Carlo

Results: symmetric configuration ($|\mathbf{k}_{J,1}| = |\mathbf{k}_{J,2}| = 35 \text{ GeV}$)

Azimuthal correlation: dependency with respect to $\mu_R = \mu_F$ and s_0 changes



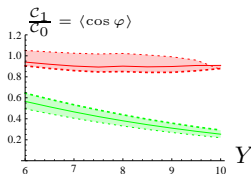
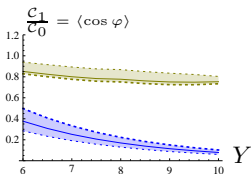
pure LL

LL vertices + imp. collinear NLL Green's fn.

NLL vertices + NLL Green's fn.

NLL vertices + imp. collinear NLL Green's fn.

Effect of changing $\mu_R = \mu_F$ by factors 2 (thick) and 1/2 (thin)

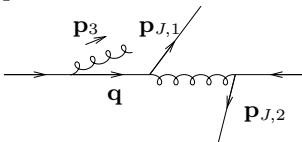


Effect of changing $\sqrt{s_0}$ by factors 2 (thick) and 1/2 (thin)

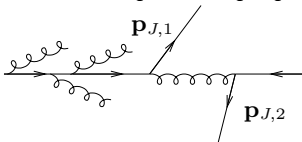
- $\langle \cos \varphi \rangle$ is still rather $\mu_R = \mu_F$ and s_0 dependent
- collinear resummation can lead to $\langle \cos \varphi \rangle > 1$ (!) for small $\mu_R = \mu_F$
- based on NLL double- ρ production (Ivanov, Papa) one can expect that small scales are disfavored (Caporale, Papa, Sabio Vera)

Motivation for asymmetric configurations

- Initial state radiation (unseen) produces divergencies if one touches the collinear singularity $\mathbf{q}^2 \rightarrow 0$

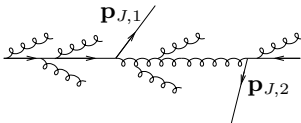


- they are compensated by virtual corrections
- this compensation is in practice difficult to implement when for some reason this additional emission is in a "corner" of the phase space (dip in the differential cross-section)
- this is the case when $\mathbf{p}_1 + \mathbf{p}_2 \rightarrow 0$
- this calls for a resummation of large remaining logs \Rightarrow **Sudakov** resummation



Motivation for asymmetric configurations

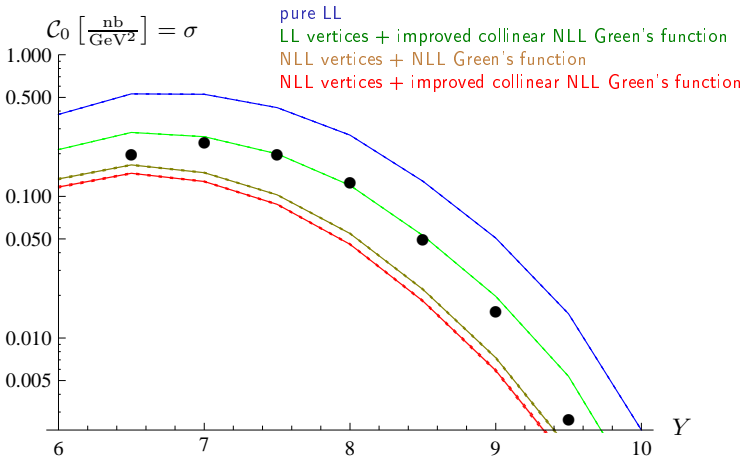
- since these resummation have never been investigated in this context, one should better avoid that region
- note that for **BFKL**, due to additional emission between the two jets, one may expect a less severe problem (at least a smearing in the dip region $|\mathbf{p}_1| \sim |\mathbf{p}_2|$)



- this may however not mean that the region $|\mathbf{p}_1| \sim |\mathbf{p}_2|$ is perfectly trustable even in a **BFKL** type of treatment
- we now investigate a region where NLL **DGLAP** is under control

Results: asymmetric configuration ($|\mathbf{k}_{J,1}| = 35 \text{ GeV}$, $|\mathbf{k}_{J,2}| = 50 \text{ GeV}$)

Cross-section

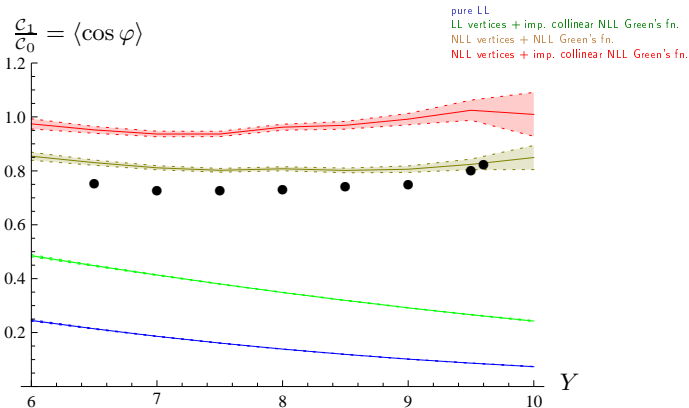


bands = errors due to the Monte Carlo integration

dots = based on the NLO DGLAP parton generator *Dijet* (thanks to M. Fontannaz)

Results: symmetric configuration ($|\mathbf{k}_{J,1}| = 35 \text{ GeV}$, $|\mathbf{k}_{J,2}| = 50 \text{ GeV}$)

Azimuthal correlation: $\langle \cos \varphi \rangle$



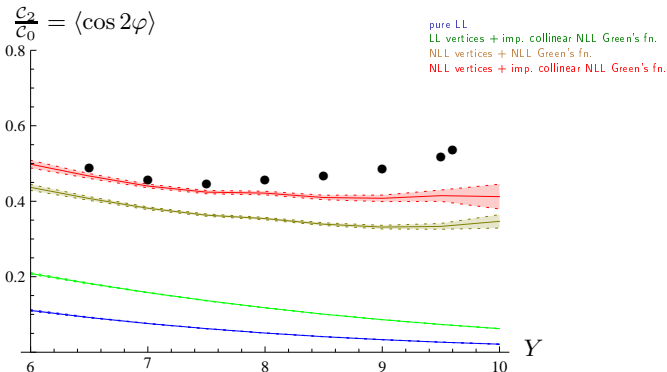
bands = errors due to the Monte Carlo integration

dots = based on the NLO DGLAP parton generator *Dijet* (thanks to M. Fontannaz)

- Both NLL and improved NLL results are almost flat in Y
- no significant difference between NLL BFKL and NLO DGLAP

Results: asymmetric configuration ($|\mathbf{k}_{J,1}| = 35 \text{ GeV}$, $|\mathbf{k}_{J,2}| = 50 \text{ GeV}$)

Azimuthal correlation: $\langle \cos 2\varphi \rangle$



bands = errors due to the Monte Carlo integration

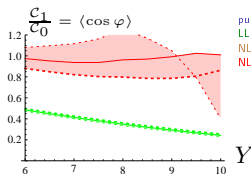
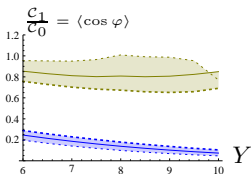
dots = based on the NLO DGLAP parton generator *Dijet* (thanks to M. Fontannaz)

Same conclusions:

- Both NLL and improved NLL results are almost flat in Y
- no significant difference between NLL BFKL and NLO DGLAP

Results: asymmetric configuration ($|\mathbf{k}_{J,1}| = 35 \text{ GeV}$, $|\mathbf{k}_{J,2}| = 50 \text{ GeV}$)

Azimuthal correlation: dependency with respect to $\mu_R = \mu_F$ and s_0 changes



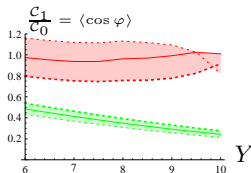
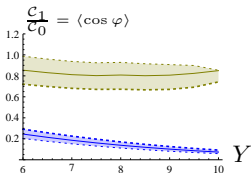
pure LL

LL vertices + imp. collinear NLL Green's fn.

NLL vertices + NLL Green's fn.

NLL vertices + imp. collinear NLL Green's fn.

Effect of changing $\mu_R = \mu_F$ by factors 2 (thick) and 1/2 (thin)



Effect of changing $\sqrt{s_0}$ by factors 2 (thick) and 1/2 (thin)

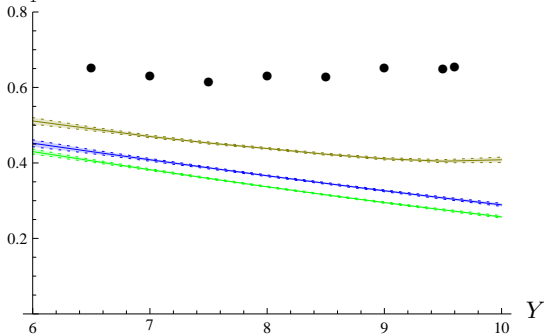
Again:

- $\langle \cos \varphi \rangle$ is still rather $\mu_R = \mu_F$ and s_0 dependent
- collinear resummation can lead to $\langle \cos \varphi \rangle > 1(!)$ for small $\mu_R = \mu_F$

Results: asymmetric configuration ($|\mathbf{k}_{J,1}| = 35 \text{ GeV}$, $|\mathbf{k}_{J,2}| = 50 \text{ GeV}$)

Ratio of azimuthal correlations $\langle \cos 2\varphi \rangle / \langle \cos \varphi \rangle$

$$\frac{c_2}{c_1} = \langle \cos 2\varphi \rangle / \langle \cos \varphi \rangle$$



pure LL

LL vertices + imp. collinear NLL Green's fn.

NLL vertices + NLL Green's fn.

NLL vertices + imp. collinear NLL Green's fn.

bands = errors due to the Monte Carlo integration

dots = based on the NLO DGLAP parton generator Dijet (thanks to Fontannaz)

NB: NLL collinear improved changed nothing wrt pure NLL

This is the only observable which might still differ noticeably between NLL BFKL and NLO DGLAP scenarii

Conclusion

- We have performed for the first time a complete NLL analysis of Mueller-Navelet jets
- the correction due to NLL jets corrections have a dramatic effect, similar to the NLL Green function corrections
- for the cross-section:
 - it makes the prediction much more stable with respect to variation of parameters (factorization scale, scale s_0 entering the rapidity definition, Parton Distribution Functions)
 - it is close to NLO DGLAP (although surprisingly a bit below!)
- the decorrelation effect is very small:
 - it is very close to NLO DGLAP
 - it is very flat in rapidity Y
 - it is still rather dependent on these parameters
- pure NLL BFKL and collinear improved NLL BFKL leads to similar results
- collinear improved NLL BFKL faces some puzzling behaviour for the azimuthal correlation
- except for $\langle \cos 2\varphi \rangle / \langle \cos \varphi \rangle$, there is almost no difference between NLL BFKL and NLO DGLAP based observables
- Mueller Navelet jets are thus probably not such a conclusive observable to see the perturbative Regge effect of QCD
- to compare with data, a serious study of Sudakov type of effects is still missing, both in DGLAP and BFKL approaches